J. Plasma Physics (2001), *vol.* 65, *part* 2, *pp.* 81–96. Printed in the United Kingdom

Two-field transport models for magnetized plasmas

O. E. GARCIA

Department of Physics, University of Tromsø,
N-9037 Tromsø, Norway

(Received 22 December 1999 and in revised form 30 June 2000)

Abstract. Two-field fluid models for low-frequency density and electrostatic potential fluctuations in a purely toroidal magnetized low-β plasma are discussed. In particular, we present some simple models suitable for investigating plasma transport close to marginal stability. For gradient-driven fluctuations, linear normal mode analysis of the interchange and resistive drift wave instabilities are reviewed, with attention to the relative phase and amplitude of density and electrostatic potential fluctuations. This reveals many characteristic features of drift-wave fluctuations that are also observed in laboratory experiments and during ionospheric irregularities. Finally, these results are used to investigate the nonlinearly conserved energy functionals, discussing the effect of magnetic field curvature and particle collisions on energy, enstrophy, and cross-correlation between density and vorticity fluctuations. Implications for turbulent fluctuations and nonlinear transport in laboratory and ionospheric plasmas are discussed.

1. Introduction

The cross-field plasma transport in many discharge experiments is observed to be anomalously large, and the enhanced transport is often caused by turbulent density and electrostatic potential fluctuations (see e.g. Endler et al. 1995; Nielsen et al. 1996; Carreras et al. 1996a; Øynes et al. 1998; Grulke et al. 1999; and references therein). The nonlinear particle flux due to fluctuations is given by $\Gamma = \widetilde{n}\widetilde{v}$, where $\widetilde{n}$ and $\widetilde{v}$ are the fluctuating plasma number density and fluid velocity respectively. For electrostatic low-frequency fluctuations, we may approximate $\widetilde{v}$ by the $\mathbf{E} \times \mathbf{B}$ drift to get the radial (x-directed) fluctuation-induced transport

$$\Gamma = -\frac{n_0 T_e}{eB}\, n \frac{\partial \varphi}{\partial y},$$

where $\varphi \equiv e\phi/T_e$ is the electrostatic potential energy perturbation normalized by the electron thermal energy T_e and $n \equiv \widetilde{n}/n_0$ is the density fluctuation normalized by the equilibrium density profile n_0. By expanding the fluctuating fields in trigonometric series, we get the non-dimensional volume-averaged radial plasma flux due to fluctuations:

$$\Gamma_n \equiv \int d\mathbf{x}\, \frac{\Gamma}{n_0 c_s} = \sum_{\mathbf{k}} i\rho_s k_y n_{\mathbf{k}} \varphi^*_{\mathbf{k}},$$

https://doi.org/10.1017/S0022377801008972 Published online by Cambridge University Press

where $c_s \equiv (T_e/m_i)^{1/2}$ is the ion acoustic velocity, $\omega_{ci} \equiv eB/m_i$ is the ion cyclotron frequency, and $\rho_s \equiv c_s/\omega_{ci}$ is the gyration radius that ions would have with electron temperature. We define the phase difference $\theta_{\mathbf{k}}$ between $\varphi_{\mathbf{k}}$ and $n_{\mathbf{k}}$ by the relation

$$\varphi_{\mathbf{k}} = \left|\frac{\varphi_{\mathbf{k}}}{n_{\mathbf{k}}}\right| n_{\mathbf{k}} \exp(i\theta_{\mathbf{k}}). \tag{1.1}$$

Using the above expression and normalizing spatial lengths by ρ_s, the flux reads

$$\Gamma_n = \sum_{\mathbf{k}\geqslant\mathbf{0}} 2k_y\, |n_{\mathbf{k}}||\varphi_{\mathbf{k}}| \sin\theta_{\mathbf{k}}. \tag{1.2}$$

This expression shows that the relative phase between density and potential fluctuations is essential for the nonlinear transport. The flux vanishes for waves exactly in phase, $\theta_{\mathbf{k}} = 0$, or in antiphase, $\theta_{\mathbf{k}} = \pi$. It is evidently maximum when the density perturbations are in phase with the poloidal electric field, which implies a phase difference between $\varphi_{\mathbf{k}}$ and $n_{\mathbf{k}}$ of $\frac{1}{2}\pi$. It is clear from the above discussion that two-field models are in general the simplest possible to self-consistently describe the qualitative features of nonlinear plasma transport.

The work presented in this paper is part of a group effort for experimental and theoretical investigation of low-frequency fluctuations in toroidal magnetized plasmas without any poloidal field component (Rypdal et al. 1994). This configuration could be called a *simple magnetized torus* (Rypdal et al. 1996) because of the simple field geometry as compared with other toroidal confinement schemes. Several devices of this type have been constructed, and have proven to be very suitable for experimental investigation of turbulent fluctuations. Here we investigate two-field models for density and electrostatic potential fluctuations, and discuss the influence of magnetic field curvature and collisions on the fluctuation characteristics and the turbulent $\mathbf{E} \times \mathbf{B}$ transport.

This paper is organized as follows. In the next section, we derive nonlinear model equations describing the essential dynamics in the experiments. Various well-known limits of the models are pointed out in Secs 3 and 4. In Sec. 3, we consider the special case of two-dimensional perturbations, and present the linear normal mode analysis for the interchange instability. An analytic non-local analysis presented in Sec. 3.2 shows that the wavelength for maximum growth rate is smaller than or of the order of the density scale length. Models for three-dimensional fluctuations are the subject of Sec. 4, where we review the linear normal mode analysis of the resistive drift-wave instability, and briefly discuss the effect of magnetic field curvature.

In the normal mode analysis the linear phase difference $\theta_{\mathbf{k}}$ and amplitude ratio $|n_{\mathbf{k}}/\varphi_{\mathbf{k}}|$ are presented and shown to be in good agreement with experimental measurements. Energy integrals conserved by the nonlinear convective terms are discussed in Sec. 5, and the sources and sinks are analysed from the viewpoint of linear stability theory. This reveals several interesting properties of magnetic field curvature and collisions. In particular, it is shown that magnetic field curvature acts as a source for enstrophy, and tends to align density and vorticity fluctuations. Conclusions are given in the last section, where it is argued that the two-field interchange model may work as a paradigm for plasma transport near marginal stability (Manheimer and Boris 1977).

2. Model equations

Motivated by the simple torus experiments, we shall assume that the magnetic field is purely toroidal. To describe a toroidal magnetized plasma, we use a cylindrical coordinate system with the major torus axis in the z direction. The magnetic field is then given by $\mathbf{B} = (B_0 R_0/R)\mathbf{b}$, where $\mathbf{b} = \mathbf{B}/B$ is a unit vector in the negative azimuthal direction, R is the radial distance from the torus axis, and B_0 is the field strength at a radial position R_0 in the plasma. The magnetic field has both a radial gradient in field strength and curvature, expressed by the relations

$$\mathbf{b} \times \boldsymbol{\nabla} \ln B = \boldsymbol{\nabla} \times \mathbf{b} = -\frac{\widehat{\mathbf{z}}}{R}.$$

2.1. Drift approximation

The momentum equation for an isothermal charged particle species α may be written in the form

$$\mathbf{v}_{\perp\alpha} = \mathbf{v}_E + \mathbf{v}_{d\alpha} + \frac{m_\alpha}{q_\alpha B}\,\mathbf{b} \times \frac{D\mathbf{v}_\alpha}{Dt} + \frac{m_\alpha \nu_{\alpha n}}{q_\alpha B}\,\mathbf{b} \times \mathbf{v}_\alpha,$$

where $\mathbf{v}_E = \mathbf{b}\times\boldsymbol{\nabla}\phi/B$ is the $\mathbf{E}\times\mathbf{B}$ drift, $\mathbf{v}_{d\alpha} = T_\alpha \mathbf{b}\times\boldsymbol{\nabla}\ln n_\alpha/q_\alpha B$ is the diamagnetic drift, $D_t \equiv \partial_t + \mathbf{v}_\alpha \cdot \boldsymbol{\nabla}$ is the convective derivative, and $\nu_{\alpha n}$ measures the rate of momentum loss due to collisions between the α-species fluid and a stationary neutral gas. For low-frequency variations, $D_t \approx \omega \ll \omega_{c\alpha}$, and magnetized plasmas, $\nu_{\alpha n} \ll \omega_{c\alpha}$, we can solve this equation for $\mathbf{v}_{\perp\alpha}$ iteratively (Shukla et al. 1984). Neglecting electron inertia, we readily obtain the lowest-order electron drift

$$\mathbf{v}_e = \mathbf{v}_E + \mathbf{v}_{de} + \frac{\nu_{en} T_e}{\omega_{ce} e B}\boldsymbol{\nabla}_\perp\left(\frac{e\phi}{T_e} - \ln n_e\right) + \frac{\omega_{ce} T_e}{\nu_{en} e B}\boldsymbol{\nabla}_{\shortparallel}\left(\frac{e\phi}{T_e} - \ln n_e\right).$$

It should be noted that in a toroidal magnetic field, the $\mathbf{E}\times\mathbf{B}$ and diamagnetic drifts are compressible:

$$\boldsymbol{\nabla}\cdot\mathbf{v}_E = -\frac{2}{BR}\,\widehat{\mathbf{z}}\cdot\boldsymbol{\nabla}\phi, \qquad \boldsymbol{\nabla}\cdot\mathbf{v}_{de} = \frac{2T_e}{eBR}\,\widehat{\mathbf{z}}\cdot\boldsymbol{\nabla}\ln n_e.$$

For the ion dynamics, we neglect diamagnetic effects and parallel drifts, but retain finite inertia corrections. First-order iteration of the inertia term then yields the ion velocity

$$\mathbf{v}_i = \mathbf{v}_E - \frac{1}{\omega_{ci} B}\frac{d\boldsymbol{\nabla}_\perp\phi}{dt} - \frac{\nu_{in}}{\omega_{ci} B}\boldsymbol{\nabla}_\perp\phi,$$

where $d_t \equiv \partial_t + \mathbf{v}_E\cdot\boldsymbol{\nabla}$. With these drifts, the ion continuity equation reads

$$\frac{d\ln n_i}{dt} - (\boldsymbol{\nabla}\ln n_i + \boldsymbol{\nabla})\cdot\left(\frac{1}{\omega_{ci}B}\frac{d\boldsymbol{\nabla}_\perp\phi}{dt} + \frac{\nu_{in}}{\omega_{ci}B}\boldsymbol{\nabla}_\perp\phi\right) - \frac{2}{BR}\,\widehat{\mathbf{z}}\cdot\boldsymbol{\nabla}\phi = 0.$$

If we further assume quasineutrality by setting $n_i \approx n_e = n$, we have a closed two-field model describing the evolution of the density n and potential ϕ. The two-field model then comprises the electron continuity equation

$$\frac{d\ln n}{dt} + (\boldsymbol{\nabla}\ln n + \boldsymbol{\nabla})\cdot\left[\frac{\nu_{en}T_e}{\omega_{ce}eB}\boldsymbol{\nabla}_\perp(\varphi - \ln n) + \frac{\omega_{ce}T_e}{\nu_{en}eB}\boldsymbol{\nabla}_{\shortparallel}(\varphi - \ln n)\right] - \frac{2T_e}{eBR}\,\widehat{\mathbf{z}}\cdot\boldsymbol{\nabla}(\varphi - \ln n) = 0, \quad (2.1a)$$

and the charge continuity equation, which is given by subtracting the electron and

https://doi.org/10.1017/S0022377801008972 Published online by Cambridge University Press

ion continuity equations,

$$(\boldsymbol{\nabla}\ln n+\boldsymbol{\nabla})\cdot\left[\frac{T_e}{\omega_{ci}eB}\frac{d\boldsymbol{\nabla}_\perp\varphi}{dt}+\frac{\nu_{in}T_e}{\omega_{ci}eB}\boldsymbol{\nabla}_\perp\varphi\right.$$
$$\left.+\frac{\nu_{en}T_e}{\omega_{ce}eB}\boldsymbol{\nabla}_\perp(\varphi-\ln n)+\frac{\omega_{ce}T_e}{\nu_{en}eB}\boldsymbol{\nabla}_{\shortparallel}(\varphi-\ln n)\right]+\frac{2T_e}{eBR}\widehat{\mathbf{z}}\cdot\boldsymbol{\nabla}\ln n=0. \quad (2.1b)$$

Here we have introduced the non-dimensional potential fluctuations $\varphi\equiv e\phi/T_e$.

The flute mode reduction of (2.1) has been solved numerically by Rypdal and co-workers (Rypdal et al. 1997, 1998; Paulsen et al. 2000) with realistic plasma sources and sinks to investigate the global properties of simple torus experiments, retaining all the effects of magnetic field curvature. Despite poor resolution this code is now producing results in qualitative agreement with experiments on the Blåmann device. In this paper, however, we shall make further simplifications, and investigate the local properties of fluctuations in inhomogeneous plasmas.

2.2. Local approximation

The model (2.1) is highly nonlinear, and further simplifications are desirable. Usually the convective part $\mathbf{v}\cdot\boldsymbol{\nabla}\ln n$ is neglected compared with the compressible part $\boldsymbol{\nabla}\cdot\mathbf{v}$ in the continuity equations. Dividing the fields into a profile and a fluctuation, e.g. $n=n_0+\widetilde{n}$, we find that the convective part can be neglected when $\widetilde{n}/n_0\approx 1/kL_n\ll 1$, where $1/L_n=|\boldsymbol{\nabla}\ln n_0|$ is the density profile scale length and k is a characteristic wavenumber for the fluctuations. Thus, neglecting the convective part as well as magnetic field curvature effects in the diffusive and inertia drifts, the model (2.1) simplifies to

$$\frac{d\ln n}{dt}+\frac{\nu_{en}T_e}{\omega_{ce}eB}\nabla_\perp^2(\varphi-\ln n)+\frac{\omega_{ce}T_e}{\nu_{en}eB}\nabla_{\shortparallel}^2(\varphi-\ln n)-\frac{2T_e}{eBR}\widehat{\mathbf{z}}\cdot\boldsymbol{\nabla}(\varphi-\ln n)=0, \quad (2.2a)$$

$$\frac{1}{\omega_{ci}}\frac{d\nabla_\perp^2\varphi}{dt}+\frac{\nu_{in}}{\omega_{ci}}\nabla_\perp^2\varphi+\frac{\nu_{en}}{\omega_{ce}}\nabla_\perp^2(\varphi-\ln n)+\frac{\omega_{ce}}{\nu_{en}}\nabla_{\shortparallel}^2(\varphi-\ln n)+\frac{2}{R}\widehat{\mathbf{z}}\cdot\boldsymbol{\nabla}\ln n=0. \quad (2.2b)$$

At this point, it is convenient to introduce dimensionless space and time variables through the Bohm normalization, $\partial_t\rightarrow\omega_{ci}\partial_t$ and $\rho_s\boldsymbol{\nabla}\rightarrow\boldsymbol{\nabla}$. Finally, we introduce a local rectangular coordinate system with the magnetic field along the z axis and x as the radial direction. In this local approximation, the dimensionless model for a weakly ionized plasma reads

$$\frac{\partial\ln n}{\partial t}+\{\varphi,\ln n\}+\nu_e\nabla_\perp^2(\varphi-\ln n)+\nu_e^{-1}\nabla_{\shortparallel}^2(\varphi-\ln n)+\zeta\frac{\partial(\ln n-\varphi)}{\partial y}=0, \quad (2.3a)$$

$$\frac{\partial\boldsymbol{\Omega}}{\partial t}+\{\varphi,\boldsymbol{\Omega}\}+\nu_i\boldsymbol{\Omega}+\nu_e\nabla_\perp^2(\varphi-\ln n)+\nu_e^{-1}\nabla_{\shortparallel}^2(\varphi-\ln n)+\zeta\frac{\partial\ln n}{\partial y}=0, \quad (2.3b)$$

where we have defined the dimensionless parameters

$$\zeta=\frac{2\rho_s}{R_0},\qquad \nu_i=\frac{\nu_{in}}{\omega_{ci}},\qquad \nu_e=\frac{\nu_{en}}{\omega_{ce}},$$

$\boldsymbol{\Omega}\equiv\nabla_\perp^2\varphi$ is the dimensionless vorticity, and we have introduced the Poisson bracket notation for the convective derivative with the $\mathbf{E}\times\mathbf{B}$ drift,

$$\mathbf{v}_E\cdot\boldsymbol{\nabla}n=\widehat{\mathbf{z}}\cdot(\boldsymbol{\nabla}\varphi\times\boldsymbol{\nabla}n)\equiv\{\varphi,n\}.$$

https://doi.org/10.1017/S0022377801008972 Published online by Cambridge University Press

Equations (2.3) are well suited for numerical simulations, studying gradient-driven fluctuations by fixing the fields to different values on some boundaries, or flux-driven fluctuations by adding source terms.

In a fully ionized plasma, the diffusive drifts due to electron–ion collisions and ion viscosity (Shukla et al. 1984) result in the model

$$\frac{\partial \ln n}{\partial t} + \{\varphi, \ln n\} + \zeta \frac{\partial (\ln n - \varphi)}{\partial y} = \nu_e^{-1} \nabla_{\shortparallel}^2 (\ln n - \varphi) + \nu_e \nabla_{\perp}^2 \ln n, \tag{2.4a}$$

$$\frac{\partial \boldsymbol{\Omega}}{\partial t} + \{\varphi, \boldsymbol{\Omega}\} + \zeta \frac{\partial \ln n}{\partial y} = \nu_e^{-1} \nabla_{\shortparallel}^2 (\ln n - \varphi) + \nu_i \nabla_{\perp}^2 \boldsymbol{\Omega}, \tag{2.4b}$$

where $\nu_e \equiv \nu_{ei}/\omega_{ce}$ and $\nu_i \equiv 3T_i \nu_{ii}/10 T_e \omega_{ci}$ are now the small dimensionless electron–ion and ion–ion collision frequencies respectively.

2.3. Exponential density profile

Dividing the density into a fluctuating part $\widetilde{n}$ and a profile $n_0(x)$, with the latter assumed to be constant in the poloidal and **B**-parallel directions we may write

$$\ln(n_0 + \widetilde{n}) = \ln\left[n_0 \left(1 + \frac{\widetilde{n}}{n_0}\right)\right] = \ln n_0 + \ln\left(1 + \frac{\widetilde{n}}{n_0}\right).$$

In the following, we shall denote the last term on the right-hand side of the above equation by n, i.e. $n \equiv \ln(1 + \widetilde{n}/n_0)$. For an exponential density profile $n_0(x) = n_{00} \exp(-x/L_n)$, the dimensionless model equations take the simple forms

$$\frac{\partial n}{\partial t} + \{\varphi, n\} + (\kappa - \zeta) \frac{\partial \varphi}{\partial y} + \zeta \frac{\partial n}{\partial y} = \nu_e \nabla_{\perp}^2 (n - \varphi) + \nu_e^{-1} \nabla_{\shortparallel}^2 (n - \varphi), \tag{2.5a}$$

$$\frac{\partial \boldsymbol{\Omega}}{\partial t} + \{\varphi, \boldsymbol{\Omega}\} + \zeta \frac{\partial n}{\partial y} + \nu_i \boldsymbol{\Omega} = \nu_e \nabla_{\perp}^2 (n - \varphi) + \nu_e^{-1} \nabla_{\shortparallel}^2 (n - \varphi), \tag{2.5b}$$

where $\kappa \equiv \rho_s / L_n$. A brief derivation of this model has previously been presented by Eickermann and Spatschek (1996). It should be noted that κ is equal to the electron diamagnetic drift and ζ to the electron gradient-B and curvature drifts, both normalized by the ion acoustic velocity c_s. We observe that both magnetic field curvature and collisions couple the equations linearly. In the following, we investigate the fluctuation characteristics described by this model.

3. Flute modes

Two-dimensional plasma turbulence has been the subject of much investigation because of its relevance to scrape-off layer physics in confinement devices (Benkadda et al. 1994; Sarazin and Ghendrih 1998), basic laboratory experiments (Nielsen et al. 1996; Rypdal et al. 1997) and equatorial irregularities (Hassam et al. 1986; LaBelle et al. 1986). The flute mode reduction of the model (2.5),

$$\frac{\partial n}{\partial t} + \{\varphi, n\} + (\kappa - \zeta) \frac{\partial \varphi}{\partial y} + \zeta \frac{\partial n}{\partial y} = \nu_e \nabla_{\perp}^2 (n - \varphi), \tag{3.1a}$$

$$\frac{\partial \boldsymbol{\Omega}}{\partial t} + \{\varphi, \boldsymbol{\Omega}\} + \zeta \frac{\partial n}{\partial y} + \nu_i \boldsymbol{\Omega} = \nu_e \nabla_{\perp}^2 (n - \varphi), \tag{3.1b}$$

has been studied by Eickermann and Spatschek (1996) and Spatschek and Eickermann (1996), with emphasis on transport close to the onset of instability. The fully

https://doi.org/10.1017/S0022377801008972 Published online by Cambridge University Press

ionized analogue of (3.1) has been solved numerically by Das et al. (1997), with periodic boundary conditions, showing an asymptotic formation of a sheared zonal flow.

Magnetic field curvature is frequently modelled as an effective gravity. Pavlenko and Weiland (1980) have derived the relevant two-field model for a collisionless plasma in a uniform magnetic field, but this model misses the $\zeta\partial_y\varphi$ term in the electron continuity equation (3.1a), which is due to the compressible $\mathbf{E}\times\mathbf{B}$ drift. It should also be noted that many investigations of the interchange instability have used a simplified model where the $\zeta\partial_y n$ term in (3.1a) is also neglected (LaBelle et al. 1986; Hassam et al. 1986; Biskamp and Schwarz 1997; Sarazin and Ghendrih 1998). The latter approximation, however, is consistent with the MHD ordering. In the following, it will be seen that these simplifications change the linear characteristics, the parameter space, and the energy integrals of the model.

Finally, we argue that characteristic of stable flute perturbations is the relation $n=\Omega$, analogous to the adiabatic electron response $n=\varphi$ for stable drift waves. The Pavlenko–Weiland model implies that $n=\Omega$ for a homogeneous plasma, while, in the absence of dissipation, the model (3.1) gives $n=\Omega$ for the threshold profile $\kappa=\zeta$. Thus, characteristic of stable flute modes are density and potential fluctuations in antiphase and relatively larger potential fluctuations at large scales, $n_{\mathbf{k}}=-k_\perp^2\varphi_{\mathbf{k}}$. Fluctuation characteristics will be discussed further below.

Neglecting cross-field dissipative effects and assuming a plane-wave solution to (2.5) of the form $\exp(i\mathbf{k}\cdot\mathbf{x}-i\omega t)$, the linearized equations are

$$(i\omega_{\rm fm}-i\omega+\nu_e^{-1}k_\parallel^2)n_{\mathbf{k}}=(i\omega_{\rm fm}-i\kappa k_y+\nu_e^{-1}k_\parallel^2)\varphi_{\mathbf{k}}, \tag{3.2a}$$

$$(i\omega_{\rm fm}+\nu_e^{-1}k_\parallel^2)n_{\mathbf{k}}=(-i\omega k_\perp^2+\nu_e^{-1}k_\parallel^2)\varphi_{\mathbf{k}}, \tag{3.2b}$$

and the dispersion relation can be written as

$$\omega^2+i\omega_{\rm dw}^2\Psi\left(\frac{\omega}{\omega_{\rm dw}}-1\right)=\omega_{\rm fm}^2\left(\frac{\omega}{\omega_{\rm fm}}-\frac{1}{\Phi}-i\frac{\omega_{\rm dw}}{\omega_{\rm fm}}\frac{\Psi}{1+k_\perp^2}\right), \tag{3.3}$$

where we have introduced the linear drift wave (dw) and flute mode (fm) frequencies

$$\omega_{\rm dw}\equiv\frac{\kappa k_y}{1+k_\perp^2},\qquad \omega_{\rm fm}\equiv\zeta k_y,$$

and the parameters

$$\Psi\equiv\nu_e^{-1}k_\parallel^2\frac{(1+k_\perp^2)^2}{\kappa k_y k_\perp^2},\qquad \Phi\equiv\frac{\zeta k_\perp^2}{\kappa-\zeta}.$$

We now investigate the linear stability as well as the phase and amplitude relation between the density and potential fluctuations of flute perturbations in a toroidal magnetic field. Some properties of non-local fluctuations are also discussed.

3.1. Normal mode analysis

The solution of the dispersion relation for the flute mode reduction ($\Psi=0$) of (3.3) reads

$$\frac{\omega}{\omega_{\rm fm}}=\frac{1}{2}\pm\left(\frac{\Phi-4}{4\Phi}\right)^{1/2}. \tag{3.4}$$

The unstable branch is presented in Fig. 1. The waves are unstable for $0<\Phi<4$, or $k_\perp^2<4(\kappa-\zeta)/\zeta$. For $\zeta>\kappa$, or equivalently $2L_n<R_0$, there are no unstable

https://doi.org/10.1017/S0022377801008972 Published online by Cambridge University Press

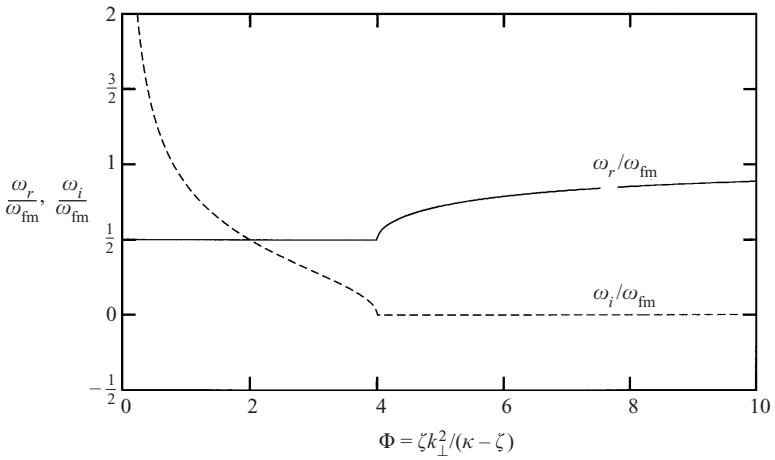

Figure 1. Dispersion diagram for unstable flute perturbations in a toroidal magnetic field. We see that the waves are unstable for $\Phi < 4$, and the phase velocity approaches the electron gradient-B and curvature drift for large Φ.

waves. This defines a threshold profile for the interchange instability. It should be noted that the linear analysis given here is the same for the gravitational instability as described by the Pavlenko–Weiland model when Φ is set equal to $\gamma k_\perp^2/\kappa$, where $\gamma \equiv g/\omega_{ci}c_s$. However, there is no stabilization for $\kappa \leqslant \zeta$ in this case, which makes equatorial spread F phenomena fundamentally different from toroidal laboratory experiments from a marginal stability point of view. For $0 < \Phi \ll 4$, the real frequency ω_r and growth rate ω_i read

$$\omega_r = \frac{\rho_s}{R_0}\, k_y, \qquad \omega_i = \left(\frac{2\rho_s^2}{L_n R_0}\right)^{1/2} \left(1 - \frac{2L_n}{R_0}\right)^{1/2} \frac{k_y}{k_\perp}. \tag{3.5}$$

Writing the spectral relation between density and potential fluctuations as in (1.1), we find from the linearized charge continuity equation (3.2b) that the density and potential fluctuations are related by

$$\frac{n_{\mathbf{k}}}{\varphi_{\mathbf{k}}} = -k_\perp^2 \left[\frac{1}{2} + \left(\frac{\Phi - 4}{4\Phi}\right)^{1/2}\right]. \tag{3.6}$$

From this expression, we may find the phase difference and amplitude ratio of the fluctuations. The phase $\theta_{\mathbf{k}}$ as function of Φ is shown in Fig. 2. We observe that stable waves are characterized by density and potential fluctuations in antiphase. Indeed, (3.6) shows that for $\Phi \gg 4$, $n_{\mathbf{k}} = -k_\perp^2 \varphi_{\mathbf{k}}$, i.e. density and vorticity fluctuations are aligned as argued previously. For the most unstable waves, $\Phi \ll 1$, the phase difference decreases towards $\frac{1}{2}\pi$, indicating large fluctuation-induced transport. Moreover, in this limit, (3.6) implies that $|n_{\mathbf{k}}/\varphi_{\mathbf{k}}| \sim k_\perp$. The fluctuation characteristics derived here from linear theory agree well with experimental measurements of turbulent plasma fluctuations driven by unstable flute modes (Huld et al. 1991; Prasad et al. 1994; Riccardi et al. 1997; Øynes et al. 1998), equatorial spread F irregularities at intermediate scales (LaBelle et al. 1986; Hysell et al. 1994), and numerical simulations (Benkadda et al. 1994; Spatschek and Eickermann 1996; Rypdal et al. 1997; Sarazin and Ghendrih 1998).

https://doi.org/10.1017/S0022377801008972 Published online by Cambridge University Press

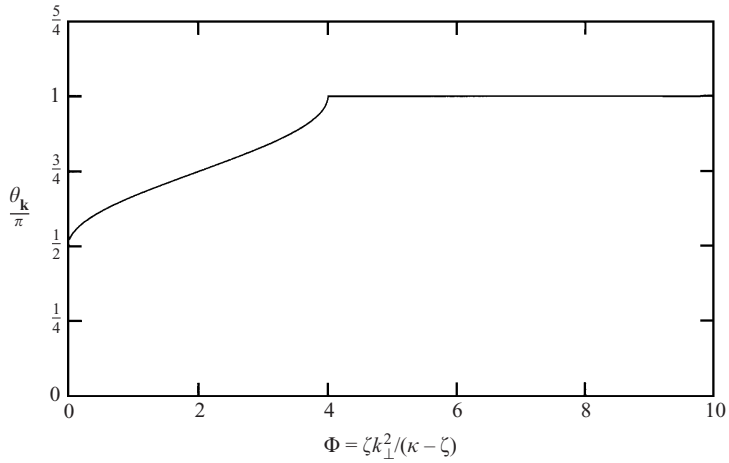

Figure 2. Linear phase difference between density and potential fluctuations for flute perturbations in a toroidal magnetic field. The stable waves are in antiphase, while for the most unstable waves, the potential lags the density by $\frac{1}{2}\pi$.

3.2. Non-local fluctuations

The local normal mode analysis shows that the largest possible wavelength for the system has the largest growth rate. Therefore we finally discuss the non-local properties for the interchange instability with an exponential density profile. Assuming a wave solution of the form $\exp(ik_y y - i\omega t)$, we readily find the linear eigenmode equation for the electrostatic potential from (2.1):

$$\frac{d^2\varphi}{dx^2} - \kappa\frac{d\varphi}{dx} - k_y^2\left[1 + \frac{\zeta(\kappa-\zeta)}{\omega(\omega-\zeta k_y)}\right]\varphi = 0.$$

In the absence of any radial structure, $d_x\varphi = 0, d_x^2\varphi = 0$, this reduces to the local dispersion relation. The above equation has a known analytical solution when the homogeneous boundary conditions $\varphi(x=0) = \varphi(x=L_x) = 0$ are imposed,

$$\varphi(x) = \widehat{\varphi}\exp\left(\tfrac{1}{2}\kappa x\right)\sin\left(\frac{l\pi\rho_s}{L_x}x\right).$$

Here we identify the radial wavenumber $k_x = l\pi\rho_s/L_x$, where $l \in \mathbb{N}$. The frequency is given by

$$\tfrac{1}{4}\kappa^2 + k_x^2 + k_y^2\left[1 + \frac{\zeta(\kappa-\zeta)}{\omega(\omega-\zeta k_y)}\right] = 0.$$

The dispersion relation can be written in the same form as in the local case, with the parameter Φ now being given by

$$\Phi = \frac{\zeta k_\perp^2}{\kappa-\zeta}\left(1 + \frac{\kappa^2}{4k_\perp^2}\right).$$

Clearly, we recover the local dispersion relation in the limit $\kappa/k_\perp \ll 1$. In the strongly non-local limit $\kappa/k_\perp \gg 1$, we get $\Phi = \kappa\zeta/4(\kappa-\zeta)$, and (3.4) shows that the growth rate is inversely proportional to the wavelength. Thus it is clear that the growth rate is maximum for some finite $k_\perp$ when non-local effects are taken

https://doi.org/10.1017/S0022377801008972 Published online by Cambridge University Press

into account. This is consistent with previous non-local studies of the gravitational interchange instability (Satyanarayana et al. 1984; Huba 1996).

4. Resistive drift waves

For a fully ionized plasma, the analogue of the model (2.5) is

$$\frac{\partial n}{\partial t} + \{\varphi, n\} + (\kappa - \zeta)\frac{\partial \varphi}{\partial y} + \zeta\frac{\partial n}{\partial y} = \nu_e^{-1}\nabla_{\shortparallel}^2(n - \varphi) + \nu_e\nabla_{\perp}^2 n, \tag{4.1a}$$

$$\frac{\partial \boldsymbol{\Omega}}{\partial t} + \{\varphi, \boldsymbol{\Omega}\} + \zeta\frac{\partial n}{\partial y} = \nu_e^{-1}\nabla_{\shortparallel}^2(n - \varphi) + \nu_i\nabla_{\perp}^2\boldsymbol{\Omega}. \tag{4.1b}$$

This model including magnetic shear in a cylindrical geometry has been extensively studied by Wakatani and co-workers, with emphasis on stellarator geometry (Wakatani et al. 1992). Closely related two-field models for edge and scrape off layer fluctuations in tokamaks and stellarators have been studied by Carreras et al. (1987), Pogutse et al. (1994), and Beyer and co-workers (Beyer and Spatschek 1996; Beyer et al. 1999). In the absence of magnetic field curvature and cross-field dissipation, (4.1) reduce to the well-known Hasegawa–Wakatani model for resistive drift waves (Hasegawa and Wakatani 1983):

$$\frac{\partial n}{\partial t} + \{\varphi, n\} + \kappa\frac{\partial \varphi}{\partial y} = \nu_e^{-1}\nabla_{\shortparallel}^2(n - \varphi), \tag{4.2a}$$

$$\frac{\partial \boldsymbol{\Omega}}{\partial t} + \{\varphi, \boldsymbol{\Omega}\} = \nu_e^{-1}\nabla_{\shortparallel}^2(n - \varphi). \tag{4.2b}$$

In the limit of adiabatic electron response to **B**-parallel electric fields, $n = \varphi$, this reduces to the Hasegawa–Mima equation (Hasegawa and Mima 1977).

4.1. Normal mode analysis

The solution of the dispersion relation for resistive drift waves in a uniform magnetic field may be written as

$$\frac{\omega}{\omega_{\mathrm{dw}}} = \frac{i\boldsymbol{\Psi}}{2}\left[-1 \pm \left(1 - \frac{i4}{\boldsymbol{\Psi}}\right)^{1/2}\right]. \tag{4.3}$$

The dispersion curves for the unstable branch are shown in Fig. 3.

In the weakly collisional or small-parallel-wavelength regime where $\nu_e^{-1}k_{\shortparallel}^2 \gg \omega_{\mathrm{dw}}$, the linear coupling is very strong, and potential and density fluctuations are nearly in phase. This is called the adiabatic limit, since electrons are near thermal equilibrium and respond adiabatically to the potential fluctuations. Expanding the square root in (4.3) to second order in the small parameter $1/\boldsymbol{\Psi}$ gives the dispersion relation for the unstable wave:

$$\frac{\omega}{\omega_{\mathrm{dw}}} = 1 + \frac{i}{\boldsymbol{\Psi}} = 1 + i\frac{\kappa k_y k_{\perp}^2}{\nu_e^{-1}k_{\shortparallel}^2\left(1 + k_{\perp}^2\right)^2}.$$

Thus the growth rate decreases rapidly with increasing $\nu_e^{-1}k_{\shortparallel}^2$ and is much smaller than the real frequency. We also note that the growth rate is largest for $k_x = 0$ and $k_y \approx 1$.

In the opposite limit, we have $\nu_e^{-1}k_{\shortparallel}^2 \ll \omega_{\mathrm{dw}}$, and the parallel wavelength is very

https://doi.org/10.1017/S0022377801008972 Published online by Cambridge University Press

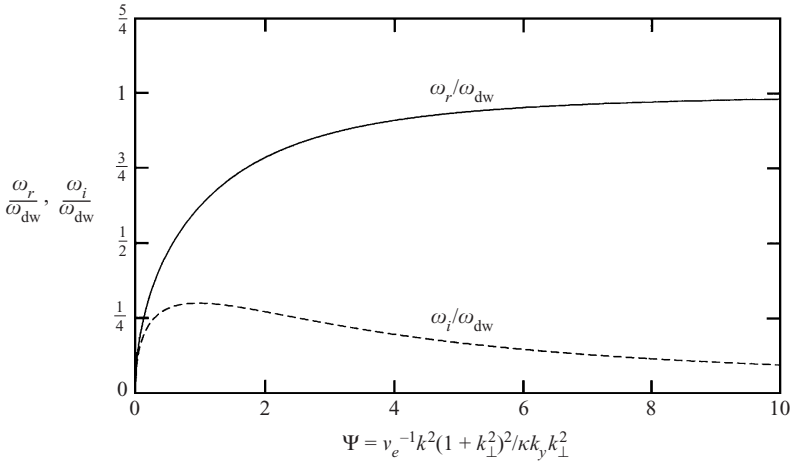

Figure 3. Dispersion diagram for resistive drift waves in a uniform magnetic field. We see that the maximum growth rate occurs at $\Psi \approx 1$ and is about one-quarter of the linear drift-wave frequency.

long or collisions are very frequent, so electrons are not able to flow along the magnetic field lines to cancel build-up of space charges. This is called the hydrodynamic regime, and the dynamics of the drift-wave turbulence is fundamentally different from that described by the Hasegawa–Mima equation. The unstable branch of the dispersion relation in this limit reduces to

$$\frac{\omega}{\omega_{dw}} = (1+i)(\tfrac{1}{2}\Psi)^{1/2} = (1+i)(1+k_\perp^2)\left(\frac{\nu_e^{-1}k_{||}^2}{2\kappa k_y k_\perp^2}\right)^{1/2}.$$

In this regime, the growth rate is of the same magnitude as the real frequency, and increases with the parallel diffusion rate $\nu_e^{-1}k_{||}^2$.

The charge continuity equation (3.2b) gives the linear relation between density and potential fluctuations as

$$\frac{n_{\mathbf{k}}}{\varphi_{\mathbf{k}}} = 1 - i\omega\frac{k_\perp^2}{\nu_e^{-1}k_{||}^2} = 1 + \frac{1+k_\perp^2}{\Psi}\left(\frac{\omega_i}{\omega_{dw}} - i\frac{\omega_r}{\omega_{dw}}\right). \tag{4.4}$$

The linear phase difference between density and potential fluctuations for $k_\perp^2 \ll 1$ is presented in Fig. 4. In the adiabatic regime, the fluctuations are in phase and have the same amplitudes. In the hydrodynamic limit, the density perturbations exceed the potential perturbations, while the phase difference increases to $\frac{1}{4}\pi$. These fluctuation characteristics are in excellent agreement with experimental observations (Hendel et al. 1968; Riccardi et al. 1997) and numerical simulations (Wakatani et al. 1992; Camargo et al. 1995).

4.2. Effect of magnetic field curvature

We now briefly discuss the effect of magnetic field curvature on the linear characteristics of resistive drift waves. As is clear from Sec. 3.1, the flute mode $k_{||} = 0$ will now also be unstable; however, field line curvature also effects the modes with finite

https://doi.org/10.1017/S0022377801008972 Published online by Cambridge University Press

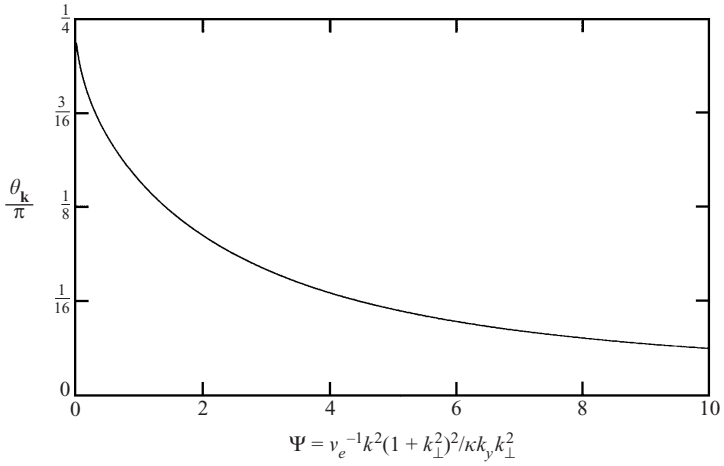

Figure 4. Linear phase relation $\theta_{\mathbf{k}}$ between density and potential fluctuations for resistive drift waves in a uniform magnetic field for wavenumbers $k_\perp^2 \ll 1$. We observe that the fluctuations are in phase in the adiabatic regime, while the phase angle increases towards $\frac{1}{4}\pi$ in the hydrodynamic limit.

$k_\parallel$. The solution of the dispersion relation (3.3) can be shown to have the form

$$2\frac{\omega}{\omega_{\mathrm{dw}}} = \frac{\omega_{\mathrm{fm}}}{\omega_{\mathrm{dw}}} - i\Psi \pm \left(i4\Psi - \Psi^2 - \frac{4-\Phi}{\Phi}\frac{\omega_{\mathrm{fm}}^2}{\omega_{\mathrm{dw}}^2} \right)^{1/2}, \tag{4.5}$$

For $\Psi = 0$, we get (3.4) and for $\omega_{\mathrm{fm}} = 0$, we get (4.3). Consider now Φ so small that the last term in the parentheses in (4.5) dominates. This yields the dispersion relation for the unstable branch:

$$2\frac{\omega}{\omega_{\mathrm{dw}}} = \frac{\omega_{\mathrm{fm}}}{\omega_{\mathrm{dw}}} + 2\Psi\left(\frac{\Phi}{4-\Phi}\right)^{1/2}\frac{\omega_{\mathrm{dw}}}{\omega_{\mathrm{fm}}} - i\Psi + i\left(\frac{4-\Phi}{\Phi}\right)^{1/2}\frac{\omega_{\mathrm{fm}}}{\omega_{\mathrm{dw}}} + \frac{i}{2}\Psi^2\left(\frac{\Phi}{4-\Phi}\right)^{1/2}\frac{\omega_{\mathrm{dw}}}{\omega_{\mathrm{fm}}}.$$

In the hydrodynamic regime, the drift modes with finite but small Ψ clearly have smaller growth rate than the flute modes.

In the adiabatic limit, Ψ is large and the second term in the parentheses in (4.5) dominates. The dispersion relation for the unstable branch in this case reads

$$\omega = \omega_{\mathrm{dw}} + \tfrac{1}{2}\omega_{\mathrm{fm}} + \frac{i}{\Phi\Psi}\frac{\omega_{\mathrm{fm}}^2}{\omega_{\mathrm{dw}}}.$$

Thus the imaginary frequency is given by

$$\omega_i = \frac{2\rho_s^2}{L_n R_0}\left(1 - \frac{2L_n}{R_0}\right)\frac{k_y^2}{\left(1+k_\perp^2\right)\nu_e^{-1}k_\parallel^2}.$$

Again we observe the stabilizing effect of the compressible $\mathbf{E}\times\mathbf{B}$ drift, defining a profile for marginal stability at $2L_n/R_0 = 1$. The three-dimensional numerical simulations by Wakatani et al. (1992) show that this model possesses the linear characteristics of flute modes in the hydrodynamic regime. In general, experiments as well as direct numerical simulations show that the linear fluctuation characteristics are preserved in the nonlinear regime. Hence we finally use the above results to discuss the energy integrals of the local models.

https://doi.org/10.1017/S0022377801008972 Published online by Cambridge University Press

5. Nonlinearly conserved energy functionals

In this section, we shall neglect the cross-field electron dissipation in the local model (2.5):

$$\frac{\partial n}{\partial t} + \{\varphi, n\} + (\kappa - \zeta)\frac{\partial \varphi}{\partial y} + \zeta \frac{\partial n}{\partial y} = \nu_e^{-1} \nabla_{\shortparallel}^2 (n - \varphi), \tag{5.1a}$$

$$\frac{\partial \Omega}{\partial t} + \{\varphi, \Omega\} + \zeta \frac{\partial n}{\partial y} + \nu_i \Omega = \nu_e^{-1} \nabla_{\shortparallel}^2 (n - \varphi). \tag{5.1b}$$

There are four integral quantities that are conserved by the convective nonlinearities: the kinetic energy K, the potential energy P, the enstrophy U, and the cross-correlation V between density and vorticity fluctuations, defined by

$$K \equiv \frac{1}{2}\int d\mathbf{x}\, (\boldsymbol{\nabla}_\perp \varphi)^2, \qquad P \equiv \frac{1}{2}\int d\mathbf{x}\, n^2,$$
$$U \equiv \frac{1}{2}\int d\mathbf{x}\, \Omega^2, \qquad V \equiv -\int d\mathbf{x}\, n\Omega.$$

Using the trigonometric series representation for the fields n and φ, we find

$$V = \sum_{\mathbf{k}} k_\perp^2 n_{\mathbf{k}} \varphi_{\mathbf{k}}^* = \sum_{\mathbf{k} \geqslant \mathbf{0}} 2k_\perp^2 \, |n_{\mathbf{k}} \varphi_{\mathbf{k}}| \cos \theta_{\mathbf{k}}.$$

Thus the cross-correlation is positive when $n_{\mathbf{k}}$ and $\varphi_{\mathbf{k}}$ are nearly in phase, characteristic of resistive drift waves, and negative when $n_{\mathbf{k}}$ and $\varphi_{\mathbf{k}}$ are in antiphase, characteristic of flute modes. In the following, we shall analyse the evolution of these integrated quantities as determined by the linear terms in the model (5.1).

5.1. Energy conservation laws

Multiplying (5.1a) by the density n and integrating over space, assuming periodic or homogeneous boundary conditions so that all surface integrals vanish, we get the evolution equation for the potential energy:

$$\frac{dP}{dt} = (\kappa - \zeta)\Gamma_n + \nu_e^{-1} \int d\mathbf{x}\, n \boldsymbol{\nabla}_{\shortparallel}^2 (n - \varphi), \tag{5.2}$$

where Γ_n is just the integrated turbulent $\mathbf{E} \times \mathbf{B}$ plasma flux down the density gradient, given by (1.2). From the characteristic phase relations from linear theory, Γ_n will be positive, and hence the plasma inhomogeneity is a source for density fluctuations. Similarly, magnetic field curvature appears as a sink for density fluctuations. Considering the parallel dissipation term, we have

$$\Gamma_{\shortparallel}^n \equiv \nu_e^{-1} \int d\mathbf{x}\, n \nabla_{\shortparallel}^2 (n - \varphi)$$
$$= \sum_{\mathbf{k} \geqslant \mathbf{0}} -2\nu_e^{-1} k_{\shortparallel}^2 \, |n_{\mathbf{k}}|^2 \left(1 - \left|\frac{\varphi_{\mathbf{k}}}{n_{\mathbf{k}}}\right| \cos \theta_{\mathbf{k}}\right).$$

For phase differences $\theta_{\mathbf{k}}$ between $\frac{1}{2}\pi$ and π, characteristic of unstable flute modes, $\Gamma_{\shortparallel}^n$ is always negative. The linear phase relation for drift waves in a uniform magnetic field implies $0 < \cos \theta_{\mathbf{k}} \leqslant 1$; however, $|\varphi_{\mathbf{k}}/n_{\mathbf{k}}| < 1$ in this case, and we should expect collisions to generally be a sink for the potential energy; see also Fig. 5.

Multiplying (5.1b) by the potential φ and integrating gives the evolution equation

https://doi.org/10.1017/S0022377801008972 Published online by Cambridge University Press

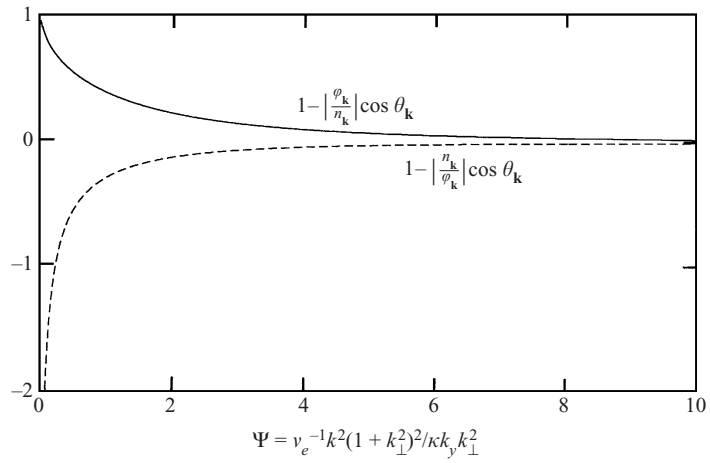

Figure 5. Linear phase and amplitude relations indicating sinks and sources for energy integrals for resistive drift waves in a uniform magnetic field in the long-wavelength limit $k_\perp^2 \ll 1$.

for the kinetic energy,

$$\frac{dK}{dt} = \zeta\Gamma_n - 2\nu_i K - \nu_e^{-1}\int d\mathbf{x}\,\varphi\boldsymbol{\nabla}_{\shortparallel}^2(n-\varphi).$$

We note that the compressible diamagnetic drift in a curved magnetic field introduces a source term for the kinetic energy. We also observe that ion–neutral collisions yield exponential decay of electric field fluctuations. To investigate the effect of electron–neutral collisions, we note that

$$\begin{aligned}\Gamma_{\shortparallel}^{\varphi} &\equiv -\nu_e^{-1}\int d\mathbf{x}\,\varphi\boldsymbol{\nabla}_{\shortparallel}^2(n-\varphi)\\ &= \sum_{\mathbf{k}\gtrless\mathbf{0}} -2\nu_e^{-1}k_{\shortparallel}^2\,|\varphi_{\mathbf{k}}|^2\left(1-\left|\frac{n_{\mathbf{k}}}{\varphi_{\mathbf{k}}}\right|\cos\theta_{\mathbf{k}}\right).\end{aligned}$$

For $\theta_{\mathbf{k}}$ between $\frac{1}{2}\pi$ and π, $\Gamma_{\shortparallel}^{\varphi}$ is negative. For phase differences smaller than $\frac{1}{2}\pi$ and $|n_{\mathbf{k}}/\varphi_{\mathbf{k}}| > 1$, characteristic of resistive drift waves in a uniform magnetic field, $\Gamma_{\shortparallel}^{\varphi}$ can become positive, as is clear from Fig. 5.

The evolution of the total energy $E \equiv K + P$ is given by

$$\frac{dE}{dt} = \kappa\Gamma_n + \Gamma_{\shortparallel} - 2\nu_i K, \tag{5.3}$$

where $\Gamma_{\shortparallel} \equiv \Gamma_{\shortparallel}^{n} + \Gamma_{\shortparallel}^{\varphi}$ is the Ohmic heat loss due to electron–neutral collisions,

$$\Gamma_{\shortparallel} = -\frac{1}{2}\nu_e^{-1}\int d\mathbf{x}\,[\boldsymbol{\nabla}_{\shortparallel}(n-\varphi)]^2.$$

Electron collisions dissipate total energy, but may also transfer energy from potential to kinetic form. We observe from (5.3) that magnetic field curvature does not enter the total energy conservation – it only transfers energy between potential and kinetic forms. Note, however, that this is not the case for the gravitational instability, where it appears as a source $\gamma\Gamma_n$ for kinetic and total energy.

5.2. Enstrophy and cross-correlation conservation laws

Multiplying (5.1b) by the vorticity Ω and integrating, we get the evolution equation for enstrophy:

$$\frac{dU}{dt} = -\zeta \int d\mathbf{x}\, \Omega \frac{\partial n}{\partial y} - 2\nu_i U + \nu_e^{-1} \int d\mathbf{x}\, \Omega \nabla_{\shortparallel}^2 (n - \varphi). \tag{5.4}$$

Again, ion–neutral collisions yield exponential damping. We now analyse the effects of curvature and electron–neutral collisions. By expanding the fields in trigonometric series, we get

$$\zeta \int d\mathbf{x}\, \Omega \frac{\partial n}{\partial y} = \sum_{\mathbf{k}} i\zeta k_y k_\perp^2 n_{\mathbf{k}}^* \varphi_{\mathbf{k}} = -\sum_{\mathbf{k} \geqslant \mathbf{0}} 2\zeta k_y k_\perp^2 \, |n_{\mathbf{k}}||\varphi_{\mathbf{k}}| \sin\theta_{\mathbf{k}}. \tag{5.5}$$

For unstable waves, $\sin\theta_{\mathbf{k}}$ is positive, and magnetic field curvature hence gives rise to a source term for enstrophy. The last term on the right-hand side of (5.4) yields

$$\nu_e^{-1} \int d\mathbf{x}\ \Omega \nabla_{\shortparallel}^2 (n - \varphi) = \sum_{\mathbf{k} \geqslant \mathbf{0}} -2\nu_e^{-1} k_{\shortparallel}^2 k_\perp^2 \, |\varphi_{\mathbf{k}}|^2 \left(1 - \left|\frac{n_{\mathbf{k}}}{\varphi_{\mathbf{k}}}\right| \cos\theta_{\mathbf{k}}\right). \tag{5.6}$$

For phase differences between $\frac{1}{2}\pi$ and π, this term is negative and represents a sink for enstrophy. However, for drift waves in a uniform magnetic field, we expect $\cos\theta_{\mathbf{k}} > 0$ and $|n_{\mathbf{k}}/\varphi_{\mathbf{k}}| > 1$, making this term positive.

Multiplying (5.1a) by Ω, (5.1b) by n, integrating over space, and adding the resulting equations gives the conservation law for the cross-correlation V:

$$\frac{dV}{dt} = \zeta \int d\mathbf{x}\, \Omega \frac{\partial n}{\partial y} - \nu_i V - \nu_e^{-1} \int d\mathbf{x}\ (n + \Omega)\, \nabla_{\shortparallel}^2 (n - \varphi). \tag{5.7}$$

The curvature term is the same as that given in (5.5), and hence is a sink for cross-correlation, i.e. curvature will tend to bring density and vorticity fluctuations in phase. This is consistent with our previous results. The effect of electron–neutral collisions depends on the relative phase and amplitude of density and potential fluctuations, and can act both as a source and as a sink for V. In a weakly ionized plasma, ion–neutral collisions will exponentially dampen any finite value of the cross-correlation. Since the cross-correlation depends on the relative phase between density and potential fluctuations, a change in ν_i may change the phase and thus implicitly affect the fluctuation-induced transport.

6. Conclusions

We have discussed two-field transport models describing low-frequency drift waves in low-β toroidally magnetized plasmas. The flute mode reduction of the most general form (2.1) describing global fluctuations has been investigated numerically by Rypdal and co-workers (Rypdal et al. 1997, 1998; Paulsen et al. 2000). The simulation results are in qualitative agreement with experimental measurements on the Blåmann device, and display all the fluctuation characteristics presented in Sec. 3.

In the case of an exponential density profile, a complete normal mode analysis has revealed fluctuation characteristics such as the relative phase and amplitude of density and electrostatic potential fluctuations. These are in good agreement with those observed in experimental measurements and numerical simulations.

https://doi.org/10.1017/S0022377801008972 Published online by Cambridge University Press

One particular feature of two-dimensional fluctuations in a curved magnetic field is their stability for $L_n < \frac{1}{2}R_0$, where L_n and R_0 are the density profile scale length and magnetic field radius of curvature respectively. Thus the compressible $\mathbf{E} \times \mathbf{B}$ drift provides a profile for marginal stability. For this reason, we believe that models such as (2.3) are well suited for investigating flux- and gradient-driven fluctuations and nonlinear transport close to marginal stability, and may work as a paradigm for describing the plasma as a self-organized critical system. It should be emphasized that the models under discussion are formulated for a considerably simpler geometry than those previously used for investigating self-organized criticality (see e.g. Carreras et al. 1996b). Moreover, the profile of marginal stability is robust to inclusion of **B**-parallel dynamics, temperature fluctuations, etc. Results from numerical simulations, along with comparisons with experimental measurements, will be presented in forthcoming contributions.

Acknowledgements

The author greatfully acknowledges discussions with K. Rypdal, J. Juul Rasmussen, H. L. Pécseli and J.-V. Paulsen. This work has been supported by the Norwegian Research Council under grant no. 125713/410.

References

Benkadda, S., Dudok de Wit, T., Verga, A., Sen, A., ASDEX Team and Garbet, X. 1994 *Phys. Rev. Lett.* **73**, 3403–3406.

Beyer, P. and Spatschek, K. H. 1996 *Phys. Plasmas* **3**, 995–1004.

Beyer, P., Sarazin, Y., Garbet, X., Ghendrih, P. and Benkadda, S. 1999 *Plasma Phys. Contr. Fusion* **41**, A757–A769.

Biskamp, D. and Schwarz, E. 1997 *Europhys. Lett.* **40**, 637–642.

Camargo, S. J., Biskamp, D. and Scott, B. D. 1995 *Phys. Plasmas* **2**, 48–62.

Carreras, B. A., Garcia, L. and Diamond, P. H. 1987 *Phys. Fluids* **30**, 1388–1400.

Carreras, B. A., Hidalgo, C., Sánchez, E., Pedrosa, M. A., Balbín, R., García-Cortés, I., van Milligen, B., Newman, D. E. and Lynch, V. E. 1996a *Phys. Plasmas* **3**, 2664–2672.

Carreras, B. A., Newman, D. E., Lynch, V. E. and Diamond, P. H. 1996b *Phys. Plasmas* **3**, 2903–2911.

Das, A., Mahajan, S., Kaw, P., Sen, A., Benkadda, S. and Verga, A. 1997 *Plasma Phys. Contr. Fusion* **4**, 1018–1027.

Eickermann, Th. and Spatschek, K. H. 1996 *Phys. Plasmas* **3**, 2869–2878.

Endler, M., Niedermeyer, H., Giannone, L., Holzhauer, E., Rudyj, A., Theimer, G., Tsois, N. and ASDEX Team 1995 *Nucl. Fusion* **35**, 1307–1339.

Grulke, O., Klinger, T. and Piel, A. 1999 *Phys. Plasmas* **6**, 788–796.

Hasegawa, A. and Mima, K. 1977 *Phys. Rev. Lett.* **39**, 205–208.

Hasegawa, A. and Wakatani, M. 1983 *Phys. Rev. Lett.* **50**, 682–686.

Hassam, A. B., Hall, W., Huba, J. D. and Keskinen, M. J. 1986 *J. Geophys. Res.* **91**, 13513–13522.

Hendel, H. W., Chu, T. K. and Politzer, P. A. 1968 *Phys. Fluids* **11**, 2426–2439.

Huba, J. D. 1996 *Phys. Plasmas* **3**, 2523–2532.

Huld, T., Nielsen, A. H., Pécseli, H. L. and Rasmussen, J. Juul 1991 *Phys. Fluids* **B3**, 1609–1625.

Hysell, D. L., Kelley, M. C., Swartz, W. E., Pfaff, R. F. and Swenson, C. M. 1994 *J. Geophys. Res.* **99**, 8827–8840.

LaBelle, J., Kelley, M. C. and Seyler, C. E. 1986 *J. Geophys. Res.* **91**, 5513–5525.

Manheimer, W. and Boris, J. P. 1977 *Comments Plasma Phys. Contr. Fusion* **3**, 15–24.

Nielsen, A. H., Pécseli, H. L. and Rasmussen, J. Juul 1996 *Phys. Plasmas* **3**, 1530–1544.

Øynes, F., Pécseli, H. and Rypdal, K. 1995 *Phys. Rev. Lett.* **75**, 81–84.

Øynes, F. J., Olsen, O. M., Pécseli, H. L., Fredriksen, Å. and Rypdal, K. 1998 *Phys. Rev.* **E57**, 2242–4255.

Paulsen, J.-V., Rypdal, R., Garcia, O. E. and Olsen, O.-M. 2000 *Physica Scripta* **T84**, 203–205.

Pavlenko, V. P. and Weiland, J. 1980 *Phys. Rev. Lett.* **44**, 148–151.

Pogutse, O., Kerner, W., Gribkov, V., Bazdenkov, S. and Osipenko, M. 1994 *Plasma Phys. Contr. Fusion* **36**, 1963–1985.

Prasad, G., Bora, D., Saxena, Y. C. and Verma, S. D. 1994 *Phys. Plasmas* **1**, 1832–1840.

Riccardi, C., Xuantong, D., Salierno, M., Gamberale, L. and Fontanesi, M. 1997 *Phys. Plasmas* **4**, 3749–3758.

Rypdal, K., Grønvoll, E., Øynes, F., Fredriksen, Å., Armstrong, R. J., Trulsen, J. and Pécseli, H. L. 1994 *Plasma Phys. Contr. Fusion* **36**, 1099–1114.

Rypdal, K., Fredriksen, H., Paulsen, J.-V. and Olsen, O. M. 1996 *Physica Scripta* **T63**, 167–173.

Rypdal, K., Garcia, O. E. and Paulsen, J.-V. 1997 *Phys. Rev. Lett.* **79**, 1857–1860.

Rypdal, K., Paulsen, J.-V. and Garcia, O. E. 1998 *Czech. J. Phys.* **48 S2**, 207–212.

Sarazin, Y. and Ghendrih, Ph. 1998 *Phys. Plasmas* **5**, 4214–4228.

Satyanarayana, P., Guzdar, P. N., Huba, J. D. and Ossakow, S. L. 1995 *J. Geophys. Res.* **89**, 2945–2954.

Shukla, P. K., Yu, M. Y., Rahman, H. U. and Spatschek, K. H. 1984 *Phys. Rep.* **105**, 227–328.

Spatschek, K. H. and Eickermann, Th. 1996 *Contrib. Plasma Phys.* **36**, 487–499.

Wakatani, M., Watanabe, K., Sugama, H. and Hasegawa, A. 1992 *Phys. Fluids* **B4**, 1754–1765.